

Short Communication

Comparative Study of the Corrosion Behaviors of Different Steels in High Performance Concrete under Marine Environment

Dongfang Zhang^{1,*}, Zhihong Fan¹, Haicheng Yang¹, Jianbo Xiong¹, Shengnian Wang¹, Qingfa Wu²

¹ Key Laboratory of Harbor & Marine Structure Durability Technology, Ministry of Transport, CCCC Fourth Harbor Engineering Institute Co., Ltd, Guangzhou, CHINA

² National Observation and Research Station of Material Corrosion and Structural Safety of Hong Kong-Zhuhai-Macao Bridge in Guangdong, Hong Kong-Zhuhai-Macao Bridge Authority, Zhuhai, CHINA

*E-mail: zhangdf8@mail.sysu.edu.cn

Received: 10 October 2022 / Accepted: 18 November 2022 / Published: 27 December 2022

The reinforced concrete structure in marine environment suffered from serious chloride-induced corrosion, which resulted in the reduction in the design life of structure. With the requirement of ultralong service life of Hong Kong-Zhuhai-Macao Bridge (120 years), stainless (SS) and epoxy coated rebar (ECR) instead of steel were used in infrastructure typically corresponding to the splash zone. However, the long-term corrosion performance of different steel in high pressure concrete under chloride attack was rare reported. Herein, both SS, EC and steel after exposed to marine environment for 3 and 7 years were comparative studied. The electro-chemical tests indicated that EC exhibited the best anti-corrosion performance with the positive open circuit potentials (OCP, -0.02 V vs CSE), lowest corrosion current density (i_{corr} , $4.41 \times 10^{-5} \mu\text{Acm}^{-2}$) and highest polarization resistance (100834 Ω). With the increasing exposed time, the OCP of steel was slightly decreased, it is probability due to the penetration of sea water to concrete. Inversely, the OCP of SS and ECR was increased. An abnormal phenomenon of SS in electrochemical impedance spectrum (EIS) was observed, the impedance of SS was much lower than that of ECR, even lower to steel. The passivation behaviors of SS and steel in concrete were further compared.

Keywords: Marine environment; High-performance concrete; Steel; Corrosion; Passivation

1. INTRODUCTION

The reinforced concrete are the most common structures that used in marine engineering, due to the good strength, versatility, durability and economy [1]. While, the corrosion behaviour of reinforcement always been observed on ports and bridges, especially in marine environment [2, 3]. The reinforcement concrete suffered with corrosion media always resulted in corrosion of steel and concrete

crack, which lead to the deterioration of structural performance directly [4]. Hong Kong-Zhuhai-Macau (HZM) sea link project as a huge concrete structure serviced in aggressive marine environment, which has ultra-long working life of 120 years [5, 6]. In order to maintain the requirement of service life, many assistant measures such as high-performance concrete [7], stainless steel [8], epoxy coated steel [9] have been used in this concrete project.

It is well known that the corrosion resistance of rebar in concrete is based on the passivation film formed during the hydration reaction. Over past years, the corrosion and passivation behaviors of steel in concrete under corrosion media have been reported in previous studies [10, 11]. Shi [12] and Lollini [13] have also studied the corrosion performance of ECR and SS in marine environment, while, these papers mainly focused on the short-term corrosion performance that resulted from accelerated corrosion test. The effect on corrosion behavior of the ECR and SS rebars by single factor resulted from the accelerated corrosion test cannot reflect the actual marine environment. Herein, the same HZM high performance concrete with steel, SS and ECR are exposed to HZM service environment for 3 and 7 years. Electrochemical technologies including open circuit potential (OCP), potentiodynamic polarization and electrochemical impedance spectroscopy (EIS) are conducted to study their long-term corrosion performances. The Mott-Schottky test and X ray photoelectron spectroscopy are used to detect the characteristic of the passivation film on rebar.

2. EXPERIMENT

2.1. Materials

The detailed information of concrete material and rebar were shown in Table 1, the parameters of different steels reinforced concrete samples were set as follow: the dimension of sample was 150mm × 150mm × 300mm, the cover thickness was 30 mm. The element composition (wt.%) of steel (HRB400) is C, 0.25; Si, 0.35; Mn, 1.36; P, 0.031; S, 0.018 and Fe balance. The element composition (wt.%) of stainless steel is C ≤ 0.08; Si ≤ 1.00; Mn ≤ 2.00; S ≤ 0.045; P ≤ 0.030; Cr, 16.00~18.00; Ni, 10.00~14.00; Mo 2.00~3.00 and Fe balance. The rebar was connected with a cooper wire in order to test conveniently, all the concrete samples were coated with epoxy resin except for the expose surface, which was expose to the marine environment (Fig. 1a and b).

Table 1. Mixture proportion and rebar type of different steels reinforced concrete samples

No.	Types	Rebar	w/c	Cement (%)	Fly ash (%)	Slag (%)	Sand (%)	Aggregate (kg/m ³)
Steel-3a	C45	Steel	0.35	40	25	35	40	2395
Steel-7a	C45	Steel	0.35	40	25	35	40	2395
SS-3a	C45	Stainless	0.35	40	25	35	40	2395
SS-7a	C45	Stainless	0.35	40	25	35	40	2395
ECR-3a	C45	Epoxy coated steel	0.35	40	25	35	40	2395
ECR-7a	C45	Epoxy coated steel	0.35	40	25	35	40	2395

2.2. Corrosion performance

The corrosion parameters of the marine environment around Hong Kong-Zhuhai-Macao Bridge was shown in Table 2. The annual average temperature and average humidity were between 22.3~23.1°C and 77~80%, respectively. The corrosion media mainly included chloride ion (Cl⁻) and sulphate ions (SO₄²⁻) with the concentration range of 10700~17020 mg/L and 1140~2260 mg/L, respectively. In addition, the pH values of sea water were varied with season, which range from 6.41 to 8.83. According to the Chinese design code GB/T50476 (CNS 2008), herein the marine environment of exposure test was classified as III-E. All the concrete samples were exposure to this environment for 3 and 7 years.

Table 2. The main characteristics of the marine environment

Temperature (°C)			Humidity (%)			Corrosion media (g/L)			CO ₂ (g/L)	pH
Average	High	Low	Average	High	Low	Cl ⁻	SO ₄ ²⁻	Mg ²⁺		
22.3~	28.4~	14.8~	77~80	100	10	3.7~	0.5~	0.2~	0.00~	6.41~
23.1	28.8	15.9				17.9	2.2	1.2	36.35	8.83

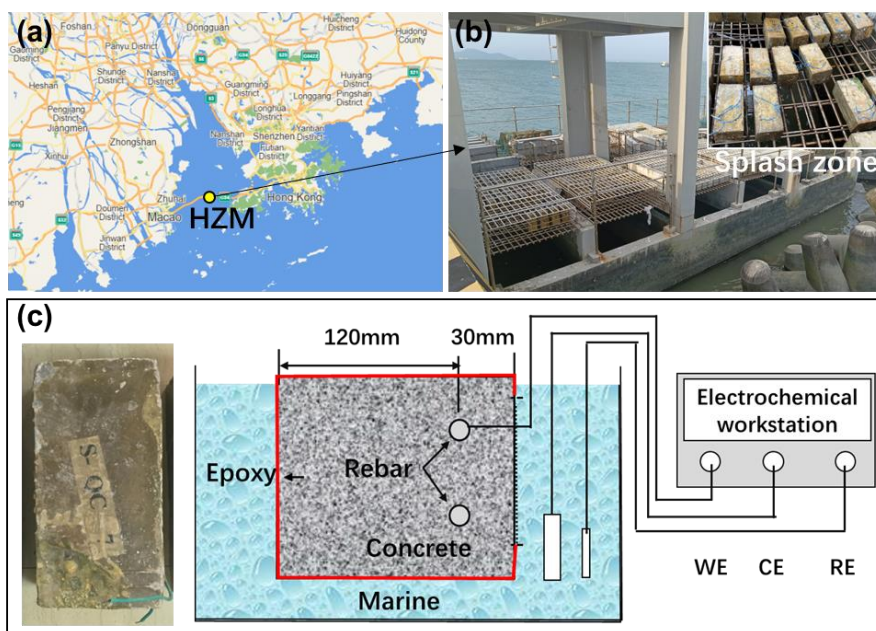


Figure 1. Geographical location of marine exposure stations in HZM (a), splash environment (b) and corrosion test illustration (c).

The concrete samples were taken back to the lab for further corrosion test after exposure for 3 and 7 years. The corrosion performance of the different steel in high pressure concrete were determined by OCP, potentiodynamic polarization and EIS in an electrolyte cell (sea water as the electrolyte). The cell consisted of a working electrode (rebar), a counter electrode (Pt) and a reference electrode (Cu/CuSO₄, CSE) with a PARASAT 2273 electrochemical workstation operated at room temperature.

The OCP measurement time was set as 600s. Potentiodynamic polarization tests were carried out at a scan rate of 0.167 mV s^{-1} . The corrosion potential (E_{corr}) and the corrosion current density (i_{corr}) were calculated using the Tafel extrapolation method. The EIS spectra were measured in a frequency range from 10 mHz to 100 kHz with a sinusoidal AC perturbation with an amplitude of 10 mV. An ac signal with a frequency of 1000 Hz and a peak-to-peak magnitude of 10mV was superimposed on the scanning potential. The capacitance (C) was calculated from the imaginary component of the impedance (Z'') using the relationship $Z'' = 1/2\pi fC$, where f is the frequency. The surface morphologies of different rebar were observed by optical microscope after electrochemical test. Passivation film of SS was investigated by X ray photoelectron spectroscopy.

3. RESULTS AND DISCUSSION

3.1. Corrosion performance

3.1.1 Open circuit potential

The OCP of different rebars were tested firstly. As shown in Fig. 2, after 3 years, the OCP curves of steel and ECR samples were nearly to a value of -100 mV. While, the SS exhibited a more negative OCP of -253 mV than other samples. The low OCP of SS was caused by the slowly passivation process on the surface of stainless steel [14]. It is well known that the stainless would form an oxide film spontaneous in the air environment. So, the passivation film of stainless steel formed in cement will take a much longer time than steel. After exposure for 7 years, the OCP of SS was significantly increased to -136 mV. And the OCP of ECR was also exhibited a much positive performance, inversely, the OCP of steel was slightly decreased to -184 mV. The potential change was corresponding to the passivation behavior. The ECR could not be passivated due to the epoxy coating, but the pore on epoxy coating will saturated with hydration products such as $\text{Ca}(\text{OH})_2$ and enhance the barrier effect. The long-term passivation of SS was contributed to the positive OCP after 7 years. The negative change of the OCP of steel from 3 to 7 years was due to the penetration of corrosion media.

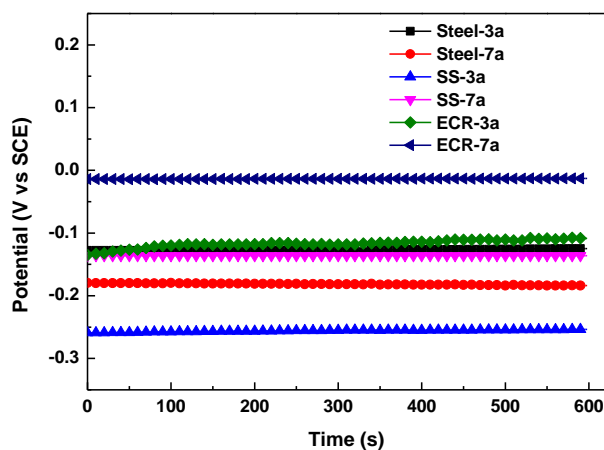


Figure 2. The OCP curves of the different steels reinforced concrete samples in marine solution at room temperature.

Table 3. Potentiodynamic measurement data of the different steels reinforced concrete samples in marine solution

Samples	OCP (V)	E_{corr} (V)	i_{corr} ($\mu\text{A}/\text{cm}^2$)
Steel-3a	-0.124	-0.152	0.162
Steel-7a	-0.184	-0.167	0.084
SS-3a	-0.253	-0.216	0.218
SS-7a	-0.136	-0.145	0.342
ECR-3a	-0.108	-0.224	4.41×10^{-5}
ECR-7a	-0.013	-0.079	2.37×10^{-5}

3.1.2 Potentiodynamic polarization test

The potentiodynamic polarization curves of the different steels reinforced concrete samples were shown in Fig. 3. The ECR samples exhibited the best corrosion resistance with the lowest i_{corr} of $4.41 \times 10^{-5} \mu\text{Acm}^{-2}$ and $2.37 \times 10^{-5} \mu\text{Acm}^{-2}$ respect to 3 and 7 years among all the samples. As revealed in OCP, the intact and insulating epoxy coating was a better barrier to corrosion media than the formed passivation film both in SS and steel. The corrosion performance of SS was similar to that of steel both in E_{corr} and i_{corr} . However, the i_{corr} of SS was slight high than that of steel, it mainly due to the slow passivation process on the SS surface. As we see, the passivated film of steel will form during 28 days. Therefore, the passivation film of steel was more thickness. According the ASTM C876 standard, the above calculated data of potentiodynamic curves indicated that all the rebar samples were in low corrosion risk.

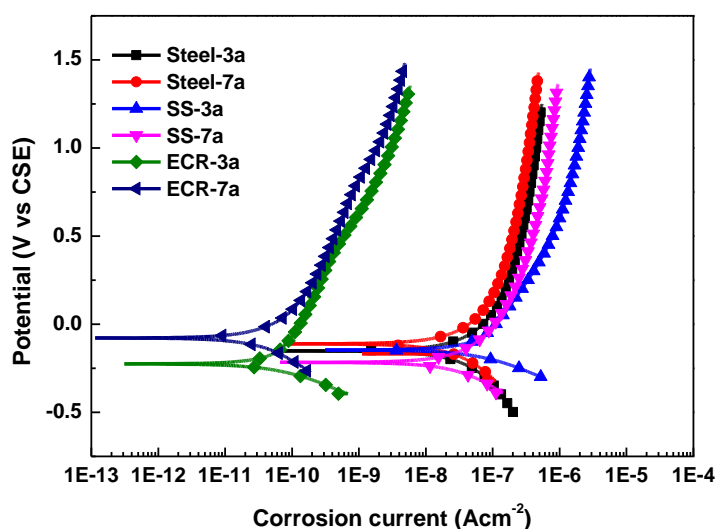


Figure 3. The potentiodynamic polarization curves of the different steels reinforced concrete samples in marine solution at room temperature.

3.1.3 The semiconductor characteristics of passivation film

In order to compare the corrosion resistance of the passivation film in steel and SS, test was applied to detect the property of passivation film [15]. The corrosion resistance of passivated film is related to its semiconductor properties, therefore, the smaller the point defect density of the passivation film is, the more difficult it is for the aggressive anions (chloride ions, etc.) to adsorb into the surface vacancy. Fig. 4 shows the Mott-Schottky curves of steel and SS rebars in high performance concrete after exposure for 7 years. The positive slope of steel indicated that the passivation film of steel was characterized with n type [16]. On the contrary, the slope of SS was negative, which indicated the passivation film was p type [17]. The N_D or N_A of passivation films was also calculated, the value of SS was one order of magnitude larger than that of steel, it indicated that the p type passivation film was much more stable in this environment.

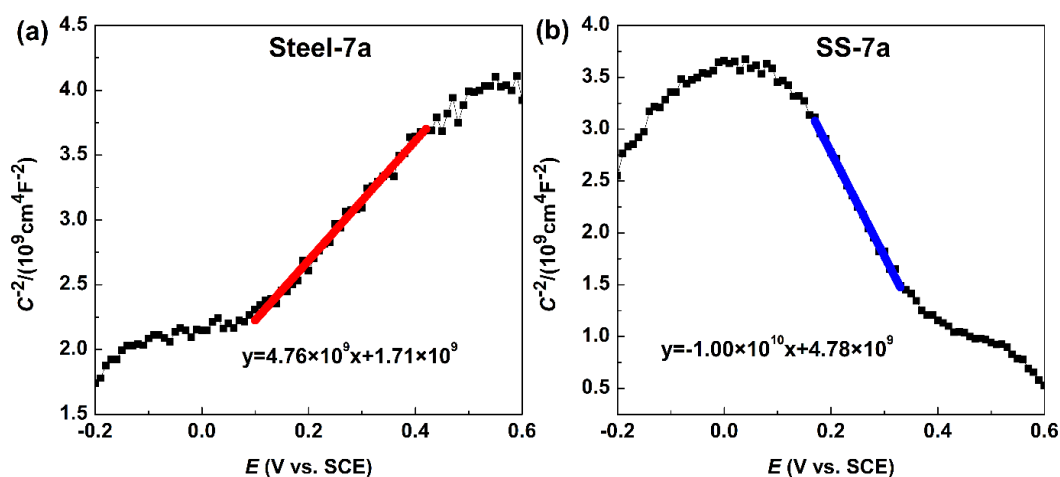


Figure 4. The Mott-Schottky plots of steel and SS in concrete after exposure for 7 years

3.1.3 Electrochemical impedance spectrum

Fig. 5 and table 4 show the EIS spectrum and fitting data of the different steels reinforced concrete samples, where R_s is the solution resistance, R_t is the charge transfer resistance, Q_t (or C_t) is the constant phase element (or capacitance), R_f is the passive film resistance or the coating resistance, Q_f is the capacitance between passive film (or coating) and concrete pore solution. The impedance of ECR was much higher than other samples, as analysed in OCP and polarization curves. As revealed in Table 4, both the steel and SS samples were exhibited a lower charge transfer resistance R_t and lower passivation film (or coating) R_f than that of the ECR samples both after 3 and 7 years. Moreover, there was a Warburg resistance occurred in the EIS spectrum of ECR samples. The EIS spectrum indicated the epoxy coating can provide a much better protection than the passivation film. Even though the impedances of SS and steel was below $10^4 \Omega$, the formation of passivation films was still enhance the corrosion resistance of rebars [15].

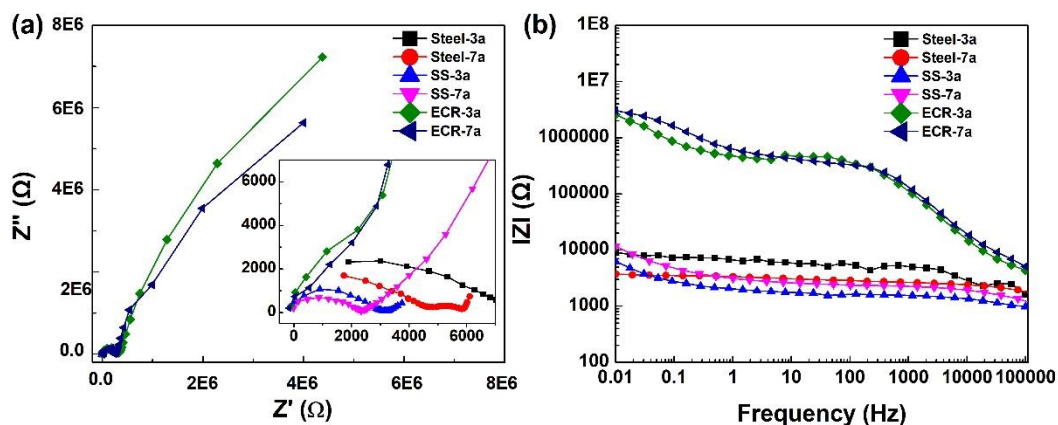


Figure 5. The EIS of the different steels reinforced concrete samples in marine solution at room temperature

Table 4. EIS fitting results of different steels in in marine solution

Samples	R_s (Ωcm^2)	R_t (Ωcm^2)	Q_t ($\Omega^{-1}\cdot\text{cm}^{-2}\cdot\text{s}^{-1}$)	n_t	R_f (Ωcm^2)	Q_f ($\Omega^{-1}\cdot\text{cm}^{-2}\cdot\text{s}^{-1}$)	n_f	Chisq
Steel-3a	100	200	1.260E-9	0.91	11892	3.614E-6	1	1.07E-4
Steel-7a	182	577	6.206E-10	0.93	9438	6.308E-7	0.96	1.21E-3
Samples	R_s (Ωcm^2)	R_t (Ωcm^2)	C_t ($\Omega^{-1}\cdot\text{cm}^{-2}\cdot\text{s}^{-1}$)		R_f (Ωcm^2)	Q_f ($\Omega^{-1}\cdot\text{cm}^{-2}\cdot\text{s}^{-1}$)	n_f	Chisq
SS-3a	100	521	4.515E-7		23651	8.618E-9	1	3.91E-3
SS-7a	100	638	5.728E-7		34352	6.214E-9	1	4.68E-3
ECR-3a	100	3786	1.198E-6		2.846E7	1.044E-9	1	2.54E-3
ECR-7a	122	4865	1.241E-9		2.986E7	5.533E-10	1	6.23E-3

3.2. Surface morphology and chemical composition

The surface morphologies of different rebars after corrosion test were further observed by optical images. As shown in Fig. 6, the corrosion products were observed on the black steel, it is contrary to the passivation behaviour revealed in polarization curves. These conflicting results were due to the anode polarization during the electrochemical test. The SS sample exhibited a stable morphology on the surface, no corrosion phenomenon was occurred, it may contribute to the stable passivation film. The surface of ECR was much more stable than other samples, the epoxy coating was still kept well gloss and intensity. However, the small crack and black site were observed on the epoxy coating after carefully detected. It is probably due to the high temperature produced by cement hydration reaction in the casting process [18]. The small crack will decrease the barrier effect of epoxy coating as the second protective film, because the bar under coating could not be passivated in concrete [19]. After exposure to marine environment for 7 years, all the rebars exhibits good anti-corrosion behaviour. both steel and SS were well passivated on the surface of rebar, the passivation film of SS was much more stable than that of the steel.

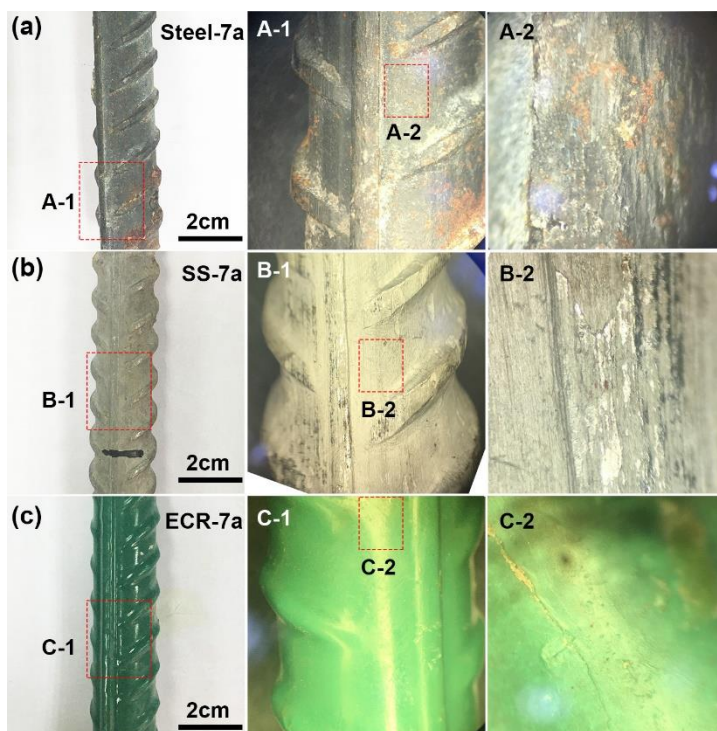


Figure 6. Surface morphologies of the different steels reinforced concrete samples after electrochemical test

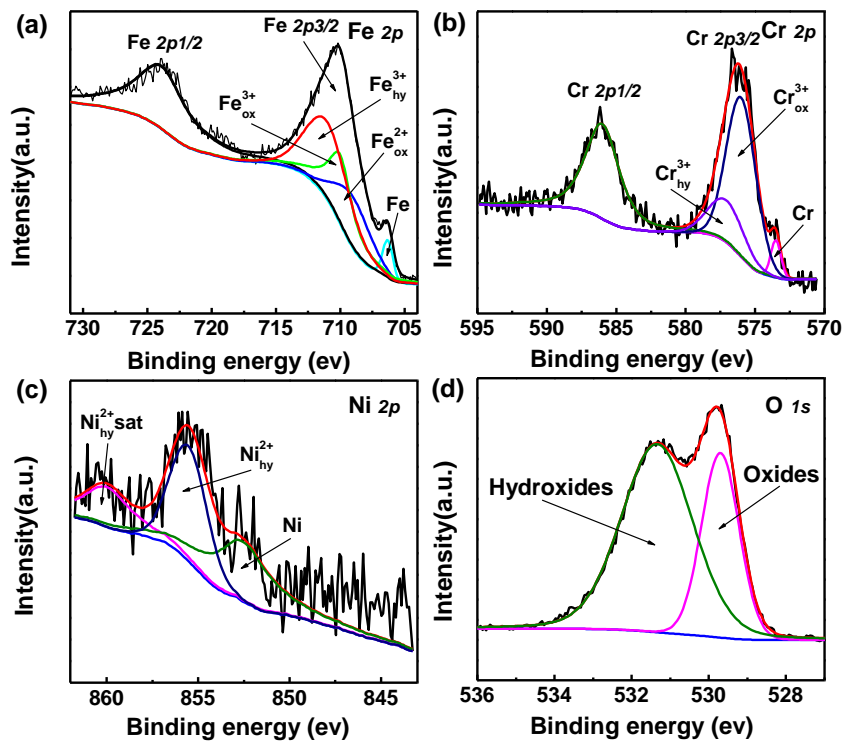


Figure 7. The X-ray photoelectron spectra of the Fe 2p, Cr 2p, Ni 2p and O 1s (b) for the passivation film of SS sample.

As illustrated in Fig. 7, Fe element was both existed in metal, oxides and hydroxides, the peaks

with binding energies of 711.6 eV are corresponding to the components of hydroxides. The other two peaks with binding energies of 710.2 eV and 709.3 eV corresponding to the Fe oxides [20], respectively. The Cr also exhibited the similar oxidation behavior on the passivation film of SS sample, as we can see in the Fig. 7b, two peaks on behalf of Cr^{3+}ox and Cr^{3+}hy were both observed [21]. In addition, a small amount of Ni oxides was also observed. It is well known that the Cr and Ni oxide helps to enhance the density and intensity of the passivation film when exposure to the aggressive chloride solution [22].

4. CONCLUSIONS

The passivation and corrosion behaviours of different rebars in high performance concrete under marine environment were comparative studied. The results indicated that the OCP and E_{corr} of rebars were slightly shift to more positive with increasing the exposure time from 3 to 7 years. The ECR exhibited the best anti-corrosion performance with the much lower i_{corr} of $10^{-5} \mu\text{Acm}^{-2}$ than steel and stainless steel. The passivation behaviour of steel was in contrast with that of SS, which characterized with a p type passivation film. The oxide and hydroxide of Cr formed in SS help to make a more stable passivation film than that of Fe.

ACKNOWLEDGEMENTS

This work was supported by a grant from the National Key R&D Program of China (No. 2019YFB1600700) and Young Talent Support Project of Guangzhou Association for Science and Technology.

References

1. M. Medeiros, A. Gobbi, G. Réus and P. Helene, *Constr. Build. Mater.*, 44 (2013) 452-457.
2. F. Qu, W. Li, W. Dong, V.W. Tam and T. Yu, *J. Build. Eng.*, 35 (2021) 102074.
3. M. Sosa, T. Pérez-López, J. Reyes, F. Corvo, R. Camacho-Chab, P. Quintana and D. Aguilar, *Int. J. Electrochem. Sci.*, 6 (2011) 6300-6318.
4. S. Muthulingam and B. Rao, *Corros. Sci.*, 82 (2014) 304-315.
5. K. Li, Q. Li, X.g. Zhou and Z. Fan, *J. Bridge Eng.*, 20 (2015) 04015001.
6. K. Li, D. Zhang, Q. Li and Z. Fan, *Cem. Concr. Res.*, 115 (2019) 545-558.
7. S. Patil, H. Somasekharaiah, H.S. Rao and V.G. Ghorpade, *Mater. Today: Proceedings*, 49 (2022) 1511-1520.
8. K. Li, P. Wang, Q. Li and Z. Fan, *Mater. Struct.*, 49 (2016) 3785-3800.
9. D.G. Manning, *Constr. Build. Mater.*, 10 (1996) 349-365.
10. P. Venkatesan, N. Palaniswamy and K. Rajagopal, *Prog. Org. Coat.* 56 (2006) 8-12.
11. N. Mohamed, M. Boulfiza and R. Evitts, *J. Mater. Eng. Perform.*, 22 (2013) 787-795.
12. X. Shi, T.A. Nguyen, Z. Suo, Y. Liu and R. Avci, *Surf. Coat. Technol.*, 204 (2009) 237-245.
13. F. Lollini, M. Carsana, M. Gastaldi and E. Redaelli, *Corros. Rev.*, 37 (2019) 3-19.
14. X. Yuan, X. Wang, Y. Cao and H. Yang, *J. Mater. Res. Technol.*, 9 (2020) 12378-12390.
15. G. Yang, Y. Du, S. Chen, Y. Ren and Y. Ma, *J. Mater. Res. Technol.*, 15 (2021) 6828-6840.
16. J. Williamson and O. Isgor, *Adv. Civ. Eng. Mater.*, 5 (2016) 80-106.
17. L. Guo, M. Lin, L. Qiao and A.A. Volinsky, *Corrosion Science*, 78 (2014) 55-62.
18. H. López-Calvo, P. Montes-Garcia, I. Kondratova, T. Bremner and M. Thomas, *Mater. Corros.*, 64 (2013) 599-608.

19. F. Tang, G. Chen, R.K. Brow, J.S. Volz and M.L. Koenigstein, *Corros. Sci.*, 59 (2012) 157-168.
20. X. Shang, Y. Zhang, N. Qu and X. Tang, *Int. J. Electrochem. Sci.*, 11 (2016) 5870-5876.
21. L. Freire, M.A. Catarino, M. Godinho, M. Ferreira, M. Ferreira, A. Simões and M. Montemor, *Cem. Concr. Compos.*, 34 (2012) 1075-1081.
22. C. Abreu, M. Cristóbal, R. Losada, X. Nóvoa, G. Pena and M. Pérez, *Electrochim. Acta*, 51 (2006) 2991-3000.

© 2022 The Authors. Published by ESG (www.electrochemsci.org). This article is an open access article distributed under the terms and conditions of the Creative Commons Attribution license (<http://creativecommons.org/licenses/by/4.0/>).